Published in final edited form as:
J Neurosci. 2012 October 3; 32(40): 13987–13999. doi:10.1523/JNEUROSCI.2433-12.2012.

TNIK is required for postsynaptic and nuclear signalling pathways and cognitive function

M.P. Coba[1,*], **N.H. Komiyama**[1,*], **J. Nithianantharajah**[1,*], **M.V. Kopanitsa**[1,6], **T. Indersmitten**[2], **N.G. Skene**[1], **E.J. Tuck**[1], **D.G. Fricker**[1], **K.A. Elsegood**[1], **L.E. Stanford**[1], **N. Afinowi**[1,6], **L.M. Saksida**[3], **T.J. Bussey**[3], **T.J. O'Dell**[4], and **S.G.N. Grant**[1,3,5]

[1]Genes to Cognition Programme, The Wellcome Trust Sanger Institute, Genome Campus, Hinxton, Cambridgeshire, CB10 1SA, UK

[2]Interdepartmental PhD Program for Neuroscience, UCLA, Los Angeles, California 90095, USA

[3]Department of Experimental Psychology, University of Cambridge, UK; The MRC and Wellcome Trust Behavioural and Clinical Neuroscience Institute, University of Cambridge, Downing St., Cambridge CB2 3EB, UK

[4]Department of Physiology, David Geffen School of Medicine at UCLA, Los Angeles, California 90095, USA

[5]Centre for Clinical Brain Sciences and Centre for Neuroregeneration, The University of Edinburgh, Chancellors Building, 47 Little France Crescent, Edinburgh EH16 4SB

[6]Synome Ltd, Babraham Research Campus, Cambridge, CB22 3AT, UK

Abstract

Traf2 and NcK interacting Kinase (TNiK) contains serine-threonine kinase and scaffold domains and has been implicated in cell proliferation and glutamate receptor regulation *in vitro*. Here we report its role *in vivo* using mice carrying a knockout mutation. TNiK binds protein complexes in the synapse linking it to the NMDA receptor (NMDAR) via AKAP9. NMDAR and metabotropic receptors bidirectionally regulate TNiK phosphorylation and TNiK was required for AMPA expression and synaptic function. TNiK also organises nuclear complexes and in the absence of TNiK, there was a marked elevation in GSK3β and phosphorylation levels of its cognate phosphorylation sites on NeuroD1 with alterations in Wnt pathway signalling. We observed impairments in dentate gyrus neurogenesis in TNiK knockout mice and cognitive testing using the touchscreen apparatus revealed impairments in pattern separation on a test of spatial discrimination. Object-location paired associates learning, which is dependent on glutamatergic signalling was also impaired. Additionally, TNiK knockout mice displayed hyperlocomotor behavior that could be rapidly reversed by GSK3β inhibitors, indicating the potential for pharmacological rescue of a behavioral phenotype. These data establish TNiK as a critical regulator of cognitive functions and suggest it may play a regulatory role in diseases impacting on its interacting proteins and complexes.

INTRODUCTION

Central to understanding the molecular basis of cognitive functions are the signalling mechanisms connecting neurotransmitter receptors to intracellular pathways regulating

Corresponding Author: Dr. S.G.N. Grant, Centre for Clinical Brain Sciences and Centre for Neuroregeneration, The University of Edinburgh, Chancellors Building, 49 Little France Crescent, Edinburgh EH16 4SB. seth.grant@ed.ac.uk. Ph: +44-131-242-7976.
*These authors contributed equally

transcription, translation and changes in electrical properties of neurons. It has become apparent that many of the proteins that participate in these pathways are physically organised within the cytoplasm into multiprotein complexes that act as molecular machines exploiting their different protein components to perform regulatory functions (Husi et al., 2000; Scott and Pawson, 2009). Within many signalling complexes are protein kinases that phosphorylate the nearby proteins and thereby orchestrate a variety of cellular functions (Scott and Pawson, 2009). How neuronal signalling complexes function is poorly understood and there are very few examples of studies where the dysfunction of signalling complexes has been studied following a mutation in the intact animal.

Toward these issues, we were intrigued by Traf2 and NcK interacting Kinase (TNiK), a protein with both scaffolding and kinase domains that had been implicated in postsynaptic signalling as well as in regulation of cell proliferation (Mahmoudi et al., 2009; Shitashige et al., 2010). TNiK is expressed in the nervous system but its role *in vivo* is currently unknown. A recent study showed that activation of *N*-methyl-D-aspartate receptors (NMDARs) regulates phosphorylation of TNiK (Coba et al., 2009). Moreover, knockdown of TNiK in primary cultured neurons decreases surface GluA1 levels (Hussain et al., 2010) and alters the synchrony of network activity (MacLaren et al., 2011), suggestive of a postsynaptic signalling function at excitatory synapses. TNiK has also been implicated in controlling dendritic outgrowth mediated by a ternary complex involving the E3 ubiquitin ligase Nedd4-1, Rap2A and TNiK (Kawabe et al., 2010). In non-neuronal cells TNiK modulates cell proliferation by regulating activation of Wnt signalling cascade through its ability to interact with β-catenin and phosphorylate the transcription factor Tcf7l2 (Mahmoudi et al., 2009; Shitashige et al., 2010). It is unknown if TNiK plays any role in neurogenesis or brain development. Finally, a link between TNiK and schizophrenia has also been suggested based on the observation that TNiK binds DISC1 (Disrupted in Schizophrenia 1) *in vitro* resulting in decreased TNiK levels and kinase activity (Wang et al., 2010). Human genetic studies have not identified mutations in TNiK, although several association studies have suggested TNiK to be involved in schizophrenia, ADHD and general cognitive function (Potkin et al., 2009; Shi et al., 2009; Elia et al., 2012).

Here we address the *in vivo* role of TNiK by examining mice carrying a knockout mutation in TNiK and show the mutations leads to dysregulation of key synaptic and nuclear signalling mechanisms. We identify complexes of proteins associated with TNiK in the postsynaptic density and the nucleus and show that the TNiK mutation has a dramatic impact on the regulation of GSK3β and phosphorylation of proteins within the complexes. We assessed the requirement of TNiK in synaptic plasticity, neuronal development and specific aspects of higher order cognitive processing using a computerised touchscreen apparatus (Bussey et al., 2011) and find evidence that TNiK plays a role in multiple cognitive functions through both synaptic and nuclear signalling pathways.

MATERIALS AND METHODS

Generation of TNiK mutant mice

The targeting vector was constructed using the AB2.2 genomic DNA BAC clone. The vector containing 6.9kb and 2.9kb of 5′ and 3′ homology arms respectively, replaced 2.6kb of TNiK genomic DNA (X28438374 to X28440972; Ensemble Build 55) containing part of exon 6 and 7 that encoded the kinase domain with IRES-lacZ-neo reporter cassette. The targeting construct was electroporated into E14TG2a ES cells. G418 (neo)-resistant clones and screened for homologous recombination by long range PCR using Expand Long Template PCR system (Roche Cat 11681842001) with PCR primer X (5′-GAGCTATTCCAGAAGTAGTGAG-3′) and primer Y (5′-CAGAGGTCTTGTCTATTCTTC -3′) that correspond to sequence in the IRES-lac-Z neo

cassette and sequence outside the 2.9kb flanking region respectively. The correctly targeted ES cells were injected into C57/BL6 blastocysts to create chimeric mice, which were bred with 129S5 mice to generate heterozygous (+/−) TNiK mutant mice. Those F1 heterozygous mice had been backcrossed with 129S5 mice for 1–2 times before being used for intercrossing. Genotyping PCR consisted of a 540bp product amplified from the wild-type (wt) allele using a forward primer A (CAACTGTCTTCTCATTAGTGG) in the wt sequence deleted by targeted mutation and a reverse primer B (GACCTGAGAGTTGTGAGCTG) downstream of the cassette. A 700bp product was amplified from the targeted allele using primer B with forward primer X, within the selection cassette. After enzymatic amplification for 35 cycles (45 seconds at 94 °C, 45 seconds at 55 °C, and 1 minute at 72 °C), the PCR products were size-fractionated on a 2% agarose gel in 1x Tris borate-EDTA buffer. Animals were treated in accordance with the UK Animal Scientific Procedures Act (1986).

Biochemical assays

PSD and nuclear fractions from mouse hippocampus were prepared using a three- step protocol as previously described (Coba et al., 2009). In brief, tissue was homogenized in ice cold buffer (10 mM Tris-HCl, pH 7.4/320 mM sucrose, 20mM β-glycerol phosphate, 1mM sodium orthovanadate, 50mM sodium fluoride) and protease inhibitors (Roche-Complete protease inhibitor cocktail). The homogenates were centrifuged at 800 × g for 10 min at 4°C and pellet resuspended in 50 mM Hepes, pH 7.4, 40 mM β-glycerol phosphate, 1mM sodium orthovanadate, 50mM sodium fluoride) and protease inhibitors (Roche-Complete protease inhibitor cocktail). The homogenates were centrifuged at 16,000 × g for 15 min at 4°C and supernatants used for nuclear extract assays. Data presented as mean ± SEM and statistical significance determined using unpaired Student's t-tests.

Hippocampal slice electrophysiology

Synaptic physiology was assessed using a multi-electrode array system and whole-cell voltage-clamp techniques as described previously (Kopanitsa et al., 2006; Carlisle et al., 2008). Eight MEA1060-BC set-ups were run in parallel and monopolar stimulation of Schäffer collateral/commissural fibres through array electrodes was performed by STG2008 stimulus generator (Multi Channel Systems, Reutlingen, FRG). For LTP experiments, a single principal recording electrode was picked in proximal part of CA1 *stratum radiatum*. To stimulate control and test pathways, two stimulation electrodes were assigned on the subicular side and on the CA3 side of *stratum radiatum* respectively. The distance from the recording electrode to the test stimulation electrode was 400–510 μm and to the control stimulation electrode 280–510 μm. To evoke orthodromic fEPSPs, test and control pathways were activated in succession at a frequency of 0.02 Hz. Baseline stimulation strength was adjusted to evoke a response that corresponded to 40% of the maximal attainable fEPSP at the recording electrode located in proximal *stratum radiatum*. Amplitude of the negative part of fEPSPs was used as a measure of the synaptic strength. To induce LTP, 10 bursts of baseline strength stimuli were administered at 5 Hz to test pathway with 4 pulses given at 100 Hz per burst (total 40 stimuli). LTP plots were scaled to the average of the first five baseline points. Normalisation of LTP values was performed by dividing the fEPSP amplitude in the tetanised pathway by the amplitude of the control fEPSP at corresponding time points. Normalised LTP values averaged across the period of 61–65 min after theta-burst stimulation were used for statistical comparison.

Paired stimulation with an interpulse interval of 50 ms was used to observe paired-pulse facilitation (PPF) in baseline conditions in the test pathway before LTP induction. PPF was calculated by dividing the negative amplitude of fEPSP obtained in response to the second pulse by the amplitude of fEPSP amplitude evoked by the preceding pulse. To assess changes in basal synaptic transmission, input-output relationships were initially compared

by mixed model repeated-measures ANOVA and Bonferroni post hoc test implemented in Prism 5 (GraphPad Software, Inc., San Diego, CA) using invidual slice data as independent observations. Since several slices were routinely recorded from every mouse, fEPSPmax, PPF and LTP values between wt and mutant mice were then compared using two-way nested ANOVA design with genotype (group) and mice (sub-group) as fixed effects. Fisher's F-statistic was calculated as Mean of $Squares_{Genotype}$/Mean of $Squares_{Residual}$ and genotype effect was considered significant if corresponding probability for the group F statistic was below 0.05.

Conventional extracellular recording techniques were used to examine the induction of LTD by 900 pulse trains of 1 Hz presynaptic fiber stimulation (Carlisle et al., 2008). For whole-cell voltage-clamp techniques, slices were bathed in an oxygenated (95% O_2 - 5% CO_2) artificial cerebrospinal fluid containing 124 mM NaCl, 2.4 mM KCl, 25 mM $NaHCO_3$, 1 mM NaH_2PO_4, 4.0 mM $CaCl_2$, 4 mM $MgSO_4$, 0.1 mM picrotoxin, and 10 mM glucose. EPSCs were recorded using electrodes were filled with a solution containing 102 mM caesium gluconate, 17.5 CsCl, 10 mM TEA-Cl, 5 mM QX314, 4.0 mM Mg-ATP, 0.3 mM Na-GTP, and 20 mM Hepes (pH = 7.2). TTX (1 μM) was added to the external solution and cells were voltage-clamped at −80 mV to record miniature EPSCs (mEPSCs). Spontaneous and miniature IPSCs (mIPSCs) were recorded using electrodes containing 140 mM CsCl, 4 mM NaCl, 1 mM MgCl2, 0,1 mM EGTA, 4 mM Mg-ATP, 0.3 mM Na-GTP, 5 mM QX314, and 10 mM HEPES (pH = 7.2). AMPA and NMDAR-mediated synaptic currents were blocked with 3.0 mM kynurenate and 1.0 μM TTX was added to the extracellular solution in experiments recording miniature IPSCs (mIPSCs). Unpaired Student's *t*-tests were used to determine statistical significance of differences between whole cell voltage clamp measurements in mutant and wt neurons.

Microarray analysis

Hippocampi (*TNiK*$^{-/-}$ n=11; wt n=33) from male and female mice aged 98–174 days were dissected and snap frozen in liquid nitrogen. RNA was extracted using a Qiagen miRNeasy kit. RNA integrity was verified using the Agilent 2100 Bioanalyzer and all samples had RIN values above 7. Unpooled samples were prepared for array analysis using the Illumina TotalPrep-96 RNA Amplification Kit and hybridized to Illumina Mouse WG-6 v2.0 Beadchips. The data was read into Bioconductor using Lumi (Du et al., 2008) and re-annotated using a previously described dataset (Barbosa-Morais et al., 2009). A Variance Stabilizing Transformation was applied followed by Quantile Normalization. Differential expression between wt and *TNiK*$^{-/-}$ mice was determined using the empirical Bayes linear model approach implemented in the Limma package (Smyth et al., 2005). Multiple hypothesis testing was corrected for using the Bonferroni-Hochberg procedure. Gene set enrichment analysis was undertaken using DAVID (Huang da et al., 2009) on those genes with adjusted $p<0.05$. The dataset has been uploaded to ArrayExpress with accession E-MTAB-1202.

Histology

For X-gal staining, free-floating sections were stained overnight in 5-bromo-4-chloro-3indolyl-β-galactoside (X-gal, Malford), mounted on pretreated slides, dehydrated and mounted with DPX mountant. For immunohistochemistry, free-floating sections were incubated in either anti-doublecortin (1:250, Cell Signalling 4604), anti-NeuroD1 (1:500, Abcam ab60704) or anti-Ki67 (1:300, Abcam ab15580). Sections were incubated with either biotinylated anti-mouse or anti-rabbit secondary antibody (1:200, DAKO) for peroxidase staining or with anti-mouse Alexa Fluor 633 or anti-rabbit Alexa Fluor 568 (1:1000) for immunofluorescence. For peroxidase staining, signal was amplified using an avidin-biotin system (Vector Laboratories) before staining in 3,3-diaminobenzidine (Dab, Sigma). For

quantitation of cell numbers, a minimum of 2 sagittal brain sections per animal was analysed from 4 pairs of *TNiK*$^{-/-}$ mice and wt littermates. Total numbers of immunopositive cells in the hippocampus were counted by an experimenter blinded to genotype and statistical significance determined using unpaired Student's t-tests.

Cognitive testing in the rodent touchscreen operant system

Testing was conducted in a touchscreen-based automated operant system that consisted of an operant chamber (21.6 × 17.8 × 12.7 cm) made of clear Perspex walls and a stainless steel grid floor, housed within a sound- and light-attenuating box (40 × 34 × 42 cm) (Med Associates, St Albans, VT). A pellet dispenser delivering 14 mg dustless pellets (BioServ, Frenchtown, NJ) into a magazine, a house light, and a tone generator was located at one end of the chamber. At the opposite end of the chamber was a flat-screen monitor equipped with an infrared touchscreen (16 × 21.2 cm) (Craft Data Limited, Chesham, UK). The touchscreen was covered by a black Perspex 'mask' that either had 6 windows (for two-choice spatial discrimination) or 3 windows (for Object-location Associative Learning) positioned in front of the touchscreen allowing the presentation of stimuli to be spatially localized and prevented the mouse from accidentally triggering the touchscreen. Stimuli presented on the screen were controlled by custom software ("MouseCat," L.M. Saksida) and responses made via nose-pokes at the stimuli were detected by the touchscreen and recorded by the software. Prior to testing, body weight of mice was slowly reduced and then maintained at or above 85% of free-feeding body weight. Animals were pre-trained through several stages, to learn to touch stimuli on the screen in order to obtain a reward as described previously (Brigman et al., 2008).

Two-choice spatial discrimination pattern separation

Adult mice (wt n=8, TniK$^{-/-}$ n=12) were initially trained to touch one of two illuminated stimuli (squares). Responses at one location (correct) resulted in a reward; responses at the other location (incorrect) resulted in a 5-s timeout (signaled by extinction of the house light). During training, the location of the two illuminated stimuli was separated by an intermediate degree of separation (2 empty/dark locations, Creer et al., 2009). Animals were required to complete 7/8 consecutive correct touches (acquisition) following which the reward contingences were reversed so that the previous incorrect location now became correct, and animals had to complete 7/8 consecutive correct touches in the other location (reversal). The correct starting location was counterbalanced between animals in each genotype and in addition, the reversal component of the task decreased the likelihood of animals developing a side bias or the use of non-spatial strategies. Mice were given a maximum of 60 trials/session/day until they reached a training criterion of completing a minimum of one acquisition and one reversal on 3 out of 4 consecutive days.

Following training, pattern separation was assessed by varying the distance between the choice locations, either situated by a high degree of separation (ie., 4 empty/dark locations between the two illuminated locations) or a low degree of separation (ie., no empty/dark location between the two illuminated locations). Mice were given unlimited trials/session/day in a 60min period and were allowed a maximum of 1 reversal. Spatial separations were held constant during each testing session per day but were varied across testing days. Mice were tested for 4 sessions on each separation, and the order of separation tested was counterbalanced between animals in each genotype across days.

Average number of trials taken to reach criterion of 7/8 consecutive correct touches for acquisition and reversal for each separation was calculated. Group differences were analyzed using either an independent samples t-test or a mixed between-within subjects analysis of variance (ANOVA) with genotype as the between-subjects factor and separation

as the within-subjects factor. A paired samples t-test was used for *post hoc* analysis to assess significant between x within-subjects interaction effect. All values reported represent mean ± standard error of the mean.

Object-Location Paired Associates Learning

Mice (wt n=8, Tnik$^{-/-}$ n=12) were tested for the ability to associate between objects (shapes) and locations on the touchscreen (Talpos et al., 2009). There were three objects (flower, plane, and spider) and three correct spatial locations (left, middle, and right, respectively). For each trial, only 2 objects were presented; one object in its correct location (S+) and the other object in one of two incorrect locations (S−). There were six possible trial types (Talpos et al., 2009), so that the flower was rewarded only when presented in the left location, the plane was rewarded only when presented in the middle location, and the spider was rewarded only when presented in the right location. A nose-poke to the correct S+ resulted in delivery of a reward and incorrect responses resulted in a 5-s time-out period, followed by correction procedure whereby the trial was repeated until the mouse made a correct choice. Nose-pokes to response windows in which no stimulus was presented were ignored. Mice were given 36 trials per session/day for 50 sessions. Group differences were analyzed using a mixed between-within subjects ANOVA with genotype as the between-subjects factor and session block as the within-subjects factor. All values reported represent mean ± standard error of the mean.

RESULTS

TNiK in glutamate receptor function *in vivo*

The TNiK gene was replaced with a *LacZ* reporter using homologous recombination in mouse embryonic stem cells (Fig. 1A, B), producing viable homozygous (*TNiK*$^{-/-}$) mice that showed no detectable TNiK protein on immunoblots of brain extracts (Fig. 1C). We observed normal Mendelian transmission in *TNiK*$^{+/-}$ intercrosses (χ^2 p=0.23) and no detectable abnormalities in body size or gross brain morphology (Fig. 1E). In wild type (wt) mice, TNiK is widely expressed in brain, including the cortex and hippocampus, where strongest staining was observed in dentate gyrus granule cells (Fig. 1D). As previously reported, TNiK protein was expressed in the PSD (Kawabe et al., 2010; Wang et al., 2010) and the nucleus (Fig. 2A)(Mahmoudi et al., 2009).

As a starting point for understanding the biochemical role of TNiK and the impact of a knockout mutation, we characterised the protein interactions and complexes formed by TNiK. Since TNiK binds DISC1 (Camargo et al., 2007; Wang et al., 2010), which binds GSK3β (Mao et al., 2009), expression of all three proteins was identified in the nucleus and in the PSD (Fig. 2A). Using immunoprecipitations (IP) from PSD extracts, these three proteins were co-isolated in NMDAR complexes (Fig. 2B) together with CRMP2 (Fig. 2C), a GSK3β substrate (Edgar et al., 2000; Nakata et al., 2003). These findings are consistent with previous reports showing that CRMP2 binds DISC1 (Camargo et al., 2007) and NMDAR GluN2B subunits (Al-Hallaq et al., 2007). How TNiK is recruited into complexes with the NMDA receptor is unknown: a direct interaction between TNiK and NMDAR subunits has not been reported in numerous yeast two-hybrid screens using NMDAR GluN1 and GluN2 subunits as bait, thus it seems likely that TNiK interacts with NMDARs via an intermediate protein. A-Kinase Anchoring protein 9 (AKAP9)(Lin et al., 1998) is a candidate since it binds TNiK (Camargo et al., 2007) and the cytoplasmic domain of GluN1. To test this, AKAP9 mutant mice were generated and characterised, and as shown in Figure 2D, TNiK's association with GluN1 was reduced to 52% ($p<0.05$) and the reverse IP confirmed this result with a 63% decrease ($p<0.05$, Fig. 2D). Since the total levels of GluN1 and TNiK remained unchanged in extracts from AKAP9 mutants (Fig. 2D) and the

interaction between TNiK and PSD-95 or GluN2B was not altered in AKAP9 mutants (Fig. 2E), these results support the view that AKAP9 links TNiK to GluN1 *in vivo*.

To understand the functional coupling of NMDAR and other glutamate receptors to TNiK, we examined the phosphorylation of S735, a proposed autophosphorylation site indicative of TNiK activity (Shitashige et al., 2010; Wang et al., 2010). In PSD extracts from hippocampal slices treated with NMDA, S735 was robustly dephosphorylated (42%, $p<0.01$). In contrast, mGluRI agonist increased S735 phosphorylation (241%, $p<0.01$) and α-amino-3-hydroxy-5-methyl-4-isoxazolepropionic acid receptor (AMPA) activation had no effect ($p>0.05$) (Fig. 2F–I). In PSD extracts of *TNiK*$^{-/-}$ mice, a decrease in AMPA receptor GluA1 levels (35% $p<0.05$, Fig. 2J) was observed, consistent with a recent report in primary cultures with TNiK knockdown (Wang et al., 2010). Since these data show biochemical interactions between TNiK and glutamate receptors, we examined excitatory and inhibitory synaptic transmission and synaptic plasticity in the hippocampus of *TNiK*$^{-/-}$ mice.

NMDAR- and AMPAR-mediated synaptic currents, long-term plasticity (LTP and LTD), and spontaneous and miniature inhibitory postsynaptic currents were normal in the hippocampal CA1 region of *TNiK*$^{-/-}$ mice (Fig. 3A–F). We noted however that evoked fEPSPs were slightly but significantly enhanced at stronger stimulation intensities compared to wild type littermates (Fig. 3B, $F_{(9,522)} = 6.48$, $P < 0.0001$). We also observed a significant increase in paired-pulse facilitation (188 ± 3% in wt compared to 196 ± 3% in TNiK$^{-/-}$ mice, $F_{1,40} = 5.36$, $p=0.026$) and a significant decrease in the frequency of AMPA receptor-mediated mEPSCs in *TNiK*$^{-/-}$ cells (*TNiK*$^{-/-}$ mice: 4.1 ± 0.5 Hz, wt: 5.3 ± 3 Hz, $p<0.05$) indicating the probability of neurotransmitter release from presynaptic terminals of excitatory synapses may be reduced in *TNiK*$^{-/-}$ mice (Fig. 3G).

Postsynaptic signalling complexes not only regulate glutamate receptor function and synaptic plasticity, but also transcriptional and other signalling pathways. Thus in the absence of a major requirement for TNiK in synaptic transmission and plasticity, and because of the previous data suggesting TNiK can regulate Wnt pathway in non-neuronal cells, we examined the requirement for TNiK in gene expression. mRNA was isolated from the hippocampus of wt and *TNiK*$^{-/-}$ mice and the transcriptome profile analysed. A total of 372 annotated genes were found to be differentially expressed with adjusted p-values <0.05 (see ArrayExpress database (http://www.ebi.ac.uk/arrayexpress) under accession number E-MTAB-1202) with many mRNAs involved in neurogenesis identified. Gene set enrichment analysis of TNiK dependent genes revealed the 3 most significantly overrepresented Gene Ontology terms related to Neurogenesis (‘regulation of neuron differentiation’ $p=0.00153$; ‘regulation of neurogenesis’ $p=0.002$; ‘regulation of nervous system development’ $p=0.0038$).

GSK3β plays a key role in regulating Wnt pathway and is physically associated with TNiK (Fig. 2C) and we asked if GSK3β was altered in *TNiK*$^{-/-}$ mice. There was a dramatic increase in GSK3β levels (143% $p<0.05$, Fig. 4A) in the PSD and nucleus, which was associated with an increase in phosphorylation of postsynaptic (CRMP2 threonine 514 increased 183% $p<0.01$; PSD-95 serine 418 and threonine 19 increased 157% $p<0.01$ and 141% $p<0.01$ respectively; Tau serine 396 increased 211% $p<0.01$, Fig. 4B) and nuclear substrates (NeuroD1 S274 increased 390% $p<0.05$, Fig. 4C). No changes were observed in the levels of GluN1, PSD-95, CRMP2, Tau, or NeuroD1 in *TNiK*$^{-/-}$ mice ($p>0.05$, Fig. 4A) and the hyperphosphorylation of the GSK3β sites on these proteins was reversed within minutes of applying a pharmacological inhibitor of GSK3β incubated on hippocampus slices (data not shown).

GSK3β antagonist reversal of locomotor hyperactivity

Spontaneous locomotor hyperactivity has been reported in mice overexpressing GSK3β (Mohn et al., 1999; Prickaerts et al., 2006; Shen et al., 2008) and we therefore tested locomotor activity in four test environments (open field, novel object exploration, elevated plus maze, locomotor activity chamber). A robust increase in locomotor activity was observed in *TNiK*$^{-/-}$ mice in all tests (Fig. 5A). Next, the ability of this effect to be rapidly reversed with a GSK3β inhibitor was tested. *TNiK*$^{-/-}$ and wt mice were placed in an activity chamber for an initial period of 30 min to assess baseline spontaneous locomotor activity where as expected, *TNiK*$^{-/-}$ mice showed significantly elevated locomotor behavior compared to wt (Fig. 5B, $p<0.001$). Within 30 minutes following administration of the GSK3β inhibitor SB216763, the locomotor activity of *TNiK*$^{-/-}$ mice was significantly reduced ($p<0.05$) to the same levels as wt mice. Furthermore, there was no significant difference between wt mice treated with vehicle or SB216763, indicating a unique sensitivity to GSK3β inhibition ($p<0.05$, Fig. 5C) was conferred by the TNiK mutation. These results suggest the mechanism underlying the locomotor phenotype in *TNiK*$^{-/-}$ mice is the result of aberrant GSK3β signalling.

TNiK is required for dentate gyrus neurogenesis

Because the S274 phosphorylation on NeuroD1 is known to inhibit its transcriptional activity (Chae et al., 2004) and NeuroD1 is required for dentate gyrus neurogenesis through Wnt signalling (Miyata et al., 1999; Kuwabara et al., 2009), and both Wnt/β-catenin defects results in loss of the dentate gyrus (Miyata et al., 1999; Liu et al., 2000), this raises the possibility that *TNiK*$^{-/-}$ mice could have dentate gyrus abnormalities. Moreover, inhibition of Wnt (Wexler et al., 2008; Clelland et al., 2009), NeuroD1 (Miyata et al., 1999) or DISC1 (Mao et al., 2009) and upregulation of GSK3β (Mao et al., 2009; Sirerol-Piquer et al., 2010) all result in impairments in dentate gyrus neurogenesis. We therefore examined neuronal cell numbers and markers of neurogenesis in the hippocampus of developing and mature mice. In young adult (6–8 week old) *TNiK*$^{-/-}$ mice there was a reduction in the numbers of dentate gyrus granule cells (29%, $p<0.001$, Fig. 6A) but no difference was observed in CA3 and CA1 pyramidal neurons (cell counts CA3 wt = 101.0±4.2, *TNiK*$^{-/-}$ = 99.6±3.9, $p=0.82$; CA1 wt = 141.5±4.4, *TNiK*$^{-/-}$ = 144.3±4.5, $p=0.66$). Examining cells expressing doublecortin (DCX), a widely used marker of adult neurogenesis and newly born neurons, and NeuroD1 (a neuronal precursor marker expressed in differentiating neurons, (von Bohlen Und Halbach, 2007), we observed significant reductions of both (DCX, 55%, $p<0.001$; NeuroD1, 41%, $p<0.001$, Fig. 6A, B). The cell proliferation marker Ki67 (Kee et al., 2002) was also reduced (70%, $p<0.01$, Fig. 6B). The decrease in dentate neurons in *TNiK*$^{-/-}$ mice was also observed by postnatal day 7 (43%, $p<0.001$) (NeuN staining, Fig. 6C) as was the reduction in cells expressing NeuroD1 (37%, $p<0.01$, Fig. 6D) and DCX (77%, $p<0.001$, Fig. 6E). Commensurate with a requirement for TNiK during these developmental stages we examined the postnatal expression profile of TNiK and found strong expression in principal excitatory neurons in all hippocampus subfields from P7 (Fig. 7).

TNiK mutants show cognitive deficits in touchscreen tests

The role of TNiK in behavior is unknown and the abnormalities in the dentate gyrus pointed to the possibility that there could be a role for TNiK in pattern separation. Pattern separation is a specific cognitive function where the ability to form distinct representations from similar inputs closely presented in space and/or time is necessary for decreasing the interference between memories. Impairments in dentate gyrus neurogenesis induced either by X-irradiation or Wnt inhibition, lead to impairments in pattern separation (Clelland et al., 2009) and conversely, enhanced pattern separation performance correlates with increased

neurogenesis (Creer et al., 2010; Sahay et al., 2011). We therefore asked if TNiK was required for pattern separation using the same two-choice spatial discrimination task in the touch-screen apparatus that was used to show the role of Wnt (Clelland et al., 2009). Mice were initially trained to discriminate the correct spatial location between two illuminated squares (located in two out of six possible locations) and then pattern separation was tested by varying the distance between the choice locations, either situated far apart (high degree of separation) or close together (low degree of separation, Fig. 6F). *TNiK*$^{-/-}$ mice showed no significant difference to wt mice during initial training (trials to training criterion: wt = 458.1±45.8, *TNiK*$^{-/-}$ = 576.3±74.2, p=0.248) and when tested with stimuli separated by a high degree of separation ($p>0.05$, Fig. 6F). However *TNiK*$^{-/-}$ mice showed a significant impairment in discrimination when the locations were in close proximity (genotype x separation interaction $p<0.01$; low separation $p<0.05$).

Previous studies have shown a reduction in dentate gyrus neurogenesis impairs pattern separation without impacting on object-location paired associates learning, which can also be measured in the touchscreen apparatus (Clelland et al., 2009). Moreover, intra-hippocampal infusions with NMDA or AMPA antagonists impair performance in this task (Talpos et al., 2009). Since TNiK is involved in NMDAR and AMPA function, it was of interest to assess object-location paired associates learning in TNiK mutants. The task measures the ability to associate three objects (flower, plane, and spider) with their correct spatial locations on the screen (left (L1), middle (L2), and right (L3), respectively (Fig. 6G). We find that *TNiK*$^{-/-}$ mice were significantly impaired in learning the association of an object and its location (effect of genotype p=0.016, Fig. 6G).

DISCUSSION

Our data provides the first direct evidence showing TNiK in the nervous system plays key roles at the synapse and nucleus, and is essential for cognition. We found that TNiK was required for two different forms of learning – pattern separation and object-location paired associates learning - that both rely on processing visual and spatial information. Pattern separation is important for keeping similar memories separate and is known to require the function of the dentate gyrus (Gilbert et al., 2001; Leutgeb et al., 2007; Bakker et al., 2008; Hunsaker and Kesner, 2008). Deletion of the essential NR1 subunit of the NMDAR specifically in dentate granule cells (McHugh et al., 2007) or disruption of neurogenesis through interference with Wnt signalling or irradiation (Clelland et al., 2009) all result in impaired pattern separation. Conversely, increased neurogenesis has been reported to correlate with enhanced pattern separation ability (Creer et al., 2010; Sahay et al., 2011). Although we observe that *TNiK*$^{-/-}$ mice show a marked impairment in neurogenesis of dentate gyrus granule cells and exhibit deficits in pattern separation, we cannot exclude the possibility that some other signalling deficit or neuroanatomical change within the granule cells might also contribute to this specific cognitive impairment. In addition to pattern separation, TNiK was required for learning object-location paired associates, which is not dependent on dentate gyrus neurogenesis (Clelland et al., 2009), but performance of this task is dependent on NMDAR and AMPAR function (Talpos et al., 2009). These findings suggest that loss of TNiK leads to additional dysfunction outside of the dentate gyrus and thus has wider cognitive impacts.

The molecular functions of TNiK are summarised in Fig. 8, highlighting a role for TNiK at both nuclear and postsynaptic complexes. Several lines of evidence indicate that TNiK mediates its role in neurogenesis through nuclear signalling complexes involving Wnt and GSK3β substrates. In the dentate gyrus subgranular zone, Wnt proteins (Grove et al., 1998; Lee et al., 2000) and β-catenin (Gao et al., 2007) are essential for neurogenesis. One of the major effectors of Wnt/β-catenin pathways is the activation of the basic helix-loop helix

(bHLH) transcription factor NeuroD1 (Kuwabara et al., 2009), and similar to Wnt/β-catenin defects, the absence of NeuroD1 during hippocampus development results in loss of the dentate gyrus (Miyata et al., 1999; Liu et al., 2000). Furthermore, in adult stages, the conditional deletion of NeuroD1 shows it is indispensable for survival and maturation of adult-born neurons (Gao et al., 2009) and defines NeuroD1 as a critical regulator of adult neurogenesis. The transcription factor activity of NeuroD1 has also been shown to be modulated by heterodimerization with the schizophrenia susceptibility gene TCF4 (Brzozka et al., 2010) and by phosphorylation of S274 by GSK3β (Chae et al., 2004), which inhibits NeuroD1 transcription activity. We found that deletion of TNiK resulted in enhanced phosphorylation of NeuroD1 S274, which would be expected to contribute to the observed reduction in neurogenesis and number of dentate gyrus neurons. Moreover, we found that NeuroD1 positive cells were decreased in the dentate gyrus of *TNiK*$^{-/-}$ mice and this decrease in precursor/progenitor cells was paralleled with a decrease in the number of newly born neurons and total number of dentate gyrus granule cells.

In non-neuronal cells, TNiK has been described as a critical component of transcriptional regulatory mechanisms, mediated by Wnt signalling, through binding and phosphorylation of the HMG box transcription factor Tcf7l2. TNiK forms a ternary complex with Tcf7l2 and β-catenin, modulating the transcriptional activation of Wnt target genes (Mahmoudi et al., 2009). In agreement with this, our results show that the deletion of TNiK results in a dysregulation of mRNAs involved in Wnt pathways. For example, CCND1 is a characteristic Wnt/β-catenin modulated gene (Mahmoudi et al., 2009) and was down regulated in the *TNiK*$^{-/-}$ mice. CCND1 was also reported to decrease as a result of DISC1 knockdown *in vivo* (Mao et al., 2009) and DISC1 and β-catenin, both TNiK interacting proteins, regulate Wnt signalling and neuronal progenitor proliferation (Kuwabara et al., 2009; Mao et al., 2009). Moreover, DISC1 induces a premature cell cycle exit and neuronal differentiation through GSK3β activity (Mao et al., 2009) and deletion of TNiK leads to an impairment in cell proliferation as demonstrated by the decrease in the total numbers of Ki67+ cells. These data indicate that TNiK is a key regulator of neurogenesis and cell proliferation through a combination of mechanisms, including modulation of transcription factor phosphorylation, activation of Wnt pathway and nuclear protein complexes.

The finding that TNiK was critical for constraining GSK3β was unexpected. In the absence of this constraint, there was increased phosphorylation of both nuclear substrates controlling cellular proliferation and synaptic substrates in the signal transduction complexes formed with scaffold proteins and glutamate receptors. GSK3β controls both neurogenesis and rapid synaptic signalling events (Jope and Roh, 2006; Beaulieu et al., 2009; Mao et al., 2009; Hur and Zhou, 2010; Sirerol-Piquer et al., 2010). Aberrant GSK3β signalling has also been implicated in and been a prominent therapeutic target (Jope and Roh, 2006; Beaulieu et al., 2009) for a variety of cognitive disorders including neuropsychiatric, neurodegenerative and more recently, neurodevelopmental disorders such as Fragile X. Interestingly, Fmr1 knockout mice show elevated GSK3β levels, aberrant neurogenesis and impairments in spatial discrimination similar to that observed in *TNiK*$^{-/-}$ mice (Min et al., 2009; Luo et al., 2010; Guo et al., 2011). This is noteworthy as Fmr1 is expressed widely in hippocampal subfields and additionally shows a phenotype where the dentate gyrus is particularly impacted, similar to that of *TNiK*$^{-/-}$ mice. Our findings support the view that TNiK acts in concert with GSK3β and DISC1 to regulate formation of neural circuits. DISC1 has been linked to Wnt signalling and neuronal progenitor proliferation (Pantelis et al., 1999; Kuwabara et al., 2009; Mao et al., 2009; Ishizuka et al., 2011) and in agreement with our biochemical data, TNiK directly binds DISC1 and β-catenin (Mahmoudi et al., 2009; Wang et al., 2010) forming complexes with GSK3β. DISC1 knockdown induces a premature cell cycle exit and neuronal differentiation through GSK3β activity (Mao et al., 2009) and TNiK knockout leads to an impairment in cell proliferation as demonstrated by the decrease in the

total numbers of Ki67+ cells. It will be important in future work, using conditional and domain specific mutations in both TNiK and GSK3β, to dissect the multifunctional roles of these interacting kinases. These genetic approaches combined with pharmacological tools will allow the developmental and cell-type specific functions to be elucidated.

We observed several relevant electrophysiological deficits in CA3-CA1 synapses of *TNiK*$^{-/-}$ mice showing a requirement for TNiK in normal excitatory synaptic function. The frequency of mEPSCs recorded in CA1 pyramidal cells of *TNiK*$^{-/-}$ mice was significantly lower than that seen in wild type cells. Decreases in mEPSC frequency can arise from a reduction in the number of excitatory synapses and/or a decrease in the probability of transmitter release from the presynaptic terminal. We found that paired-pulse facilitation in the hippocampal CA1 region was significantly enhanced in slices from *TNiK*$^{-/-}$ mice suggesting that TNiK may influence presynaptic processes involved in glutamatergic synaptic transmission. At the biochemical level, we found that TNiK was required for GluA1 expression, which is consistent with recent studies using siRNA-mediated TNiK knockdown in primary neuronal cultures (Hussain et al., 2010; Wang et al., 2010). The change in GluA1 did not appear to have a major impact on synaptic transmission as we did not observe reductions in mEPSC amplitudes or evoked AMPAR-mediated synaptic responses in hippocampal slices from *TNiK*$^{-/-}$ mice. It is not surprising that the 35% decrease in GluA1 levels in *TNiK*$^{-/-}$ mice is not associated with changes in basal synaptic transmission in the hippocampal CA1 region. For example, previous studies have found that both field excitatory postsynaptic potentials and miniature excitatory postsynaptic currents are normal in GluA1 knockout mice (Zamanillo et al., 1999; however see Andrasfalvy et al., 2003). This is most likely due to the fact that functional AMPA receptors can be made from hetero and homomeric combinations of other subunits (GluA2-4). In addition, approximately 95% of the extrasynaptic pool of AMPARs normally contain GluA1 subunits (Lu et al., 2009). Thus there is likely a considerable reserve pool of other AMPAR subunits that could compensate for the modest decrease in total GluA1 levels in TNiK mutants.

TNiK was physically linked to the NMDA receptor complex and its autophosphorylation site was regulated by both NMDAR and mGluR receptors (in opposing directions). Moreover, in the absence of TNiK there was an elevation of GSK3β phosphorylation on postsynaptic substrates. We tested several LTP and LTD protocols, which are transcription and translation-independent, and these were normal in *TNiK*$^{-/-}$ mice. We cannot rule out a potentially important role for TNiK in other forms of LTP such as transcription-dependent or translation-dependent forms of late-phase LTP, which may be relevant to the potential link with FMRP noted above.

A number of circumstantial lines of evidence suggest TNiK is involved in neuropsychiatric diseases. In addition to its interaction with DISC1, there are links between TNiK and other genes implicated in schizophrenia. NeuroD1 heterodimerizes with the schizophrenia susceptibility protein TCF4 (Brzozka et al., 2010) and TNiK forms a ternary complex with Tcf7l2 (another schizophrenia susceptibility protein, Hansen et al., 2011) and β-catenin, modulating the transcriptional activation of Wnt target genes. We find that TNiK binds and regulates glutamate receptor complexes, which are involved in a range of different cognitive disorders including schizophrenia, autism and forms of mental retardation (Fernandez et al., 2009; Bayes et al., 2011). A recent large-scale study of *de novo* copy number variation in schizophrenia found a highly significant enrichment in mutations affecting the MAGUK associated signalling complexes that include PSD-95, TNiK and proteins dependent on TNiK function (Kirov et al., 2011). We observed that loss of TNiK impairs object-location paired associates learning, which has been evaluated in humans using computer-automated tests such as the object-place paired-associate-learning (PAL) test from the Cambridge Neuropsychological Test Automated Battery (CANTAB) that is widely used in clinical

settings (Barnett et al., 2010). Moreover, schizophrenic patients show robust impairments on PAL and performance on this test correlates with symptom severity (Barnett et al., 2005; Barnett et al., 2010). Aberrant neurogenesis is also emerging as a neuropathological change in schizophrenia (Reif et al., 2006; Reif et al., 2007; Toro and Deakin, 2007; DeCarolis and Eisch, 2010) and while no study has yet explicitly examined pattern separation in schizophrenic patients, its importance as a cognitive function of potential relevance to schizophrenia has been argued (Tamminga et al., 2010). It is now emerging that human cognitive disorders arise from mutation or disruption in many postsynaptic signalling proteins, including those interacting with TNiK, and future studies may determine if TNiK plays a role in modulating these disease phenotypes.

Acknowledgments

We thank T. Ryan, C. Pettit, J. Bussell and RSF staff for technical assistance, Mike Croning for the website and G2Cdb support and members of the Genes to Cognition Programme for critical comments on the manuscript. We are grateful to M. Goedert for Tau antibodies; N. Brandon for DISC1 antibody; P. Somogyi, J. Gogos, T. W. Robbins, R. Barker and M. Caron for advice. MPC, NHK, JN, MVK, NGS, EJT, DGF, KAE, LES, NA, SGNG were supported by the Wellcome Trust, Medical Research Council (UK), European Union Seventh Framework Programme under grant agreement numbers HEALTH-F2-2009-241498 (“EUROSPIN” project), HEALTH-F2-2009-242167 (“SynSys project”) and HEALTH-F2-2009-241995 (“GENCODYS project”). MPC was also supported by Human Frontiers Science Program. TJO and TI were supported by National Institute of Mental Health (grant # MH609197).

References

Al-Hallaq RA, Conrads TP, Veenstra TD, Wenthold RJ. NMDA di-heteromeric receptor populations and associated proteins in rat hippocampus. The Journal of neuroscience: the official journal of the Society for Neuroscience. 2007; 27:8334–8343. [PubMed: 17670980]

Andrasfalvy BK, Smith MA, Borchardt T, Sprengel R, Magee JC. Impaired regulation of synaptic strength in hippocampal neurons from GluR1-deficient mice. The Journal of physiology. 2003; 552:35–45. [PubMed: 12878757]

Bakker A, Kirwan CB, Miller M, Stark CE. Pattern separation in the human hippocampal CA3 and dentate gyrus. Science (New York, NY. 2008; 319:1640–1642.

Barbosa-Morais NL, Dunning MJ, Samarajiwa SA, Darot JF, Ritchie ME, Lynch AG, Tavare S. A re-annotation pipeline for Illumina BeadArrays: improving the interpretation of gene expression data. Nucleic Acids Res. 2009; 38:e17. [PubMed: 19923232]

Barnett JH, Robbins TW, Leeson VC, Sahakian BJ, Joyce EM, Blackwell AD. Assessing cognitive function in clinical trials of schizophrenia. Neurosci Biobehav Rev. 2010; 34:1161–1177. [PubMed: 20105440]

Barnett JH, Sahakian BJ, Werners U, Hill KE, Brazil R, Gallagher O, Bullmore ET, Jones PB. Visuospatial learning and executive function are independently impaired in first-episode psychosis. Psychol Med. 2005; 35:1031–1041. [PubMed: 16045069]

Bayes A, van de Lagemaat LN, Collins MO, Croning MD, Whittle IR, Choudhary JS, Grant SG. Characterization of the proteome, diseases and evolution of the human postsynaptic density. Nat Neurosci. 2011; 14:19–21. [PubMed: 21170055]

Beaulieu JM, Gainetdinov RR, Caron MG. Akt/GSK3 signaling in the action of psychotropic drugs. Annu Rev Pharmacol Toxicol. 2009; 49:327–347. [PubMed: 18928402]

Brigman JL, Feyder M, Saksida LM, Bussey TJ, Mishina M, Holmes A. Impaired discrimination learning in mice lacking the NMDA receptor NR2A subunit. Learn Mem. 2008; 15:50–54. [PubMed: 18230672]

Brzozka MM, Radyushkin K, Wichert SP, Ehrenreich H, Rossner MJ. Cognitive and Sensorimotor Gating Impairments in Transgenic Mice Overexpressing the Schizophrenia Susceptibility Gene Tcf4 in the Brain. Biological psychiatry. 2010; 68:33–40. [PubMed: 20434134]

Bussey TJ, Holmes A, Lyon L, Mar AC, McAllister KA, Nithianantharajah J, Oomen CA, Saksida LM. New translational assays for preclinical modelling of cognition in schizophrenia: the

touchscreen testing method for mice and rats. Neuropharmacology. 2011; 62:1191–1203. [PubMed: 21530550]

Camargo LM, Collura V, Rain JC, Mizuguchi K, Hermjakob H, Kerrien S, Bonnert TP, Whiting PJ, Brandon NJ. Disrupted in Schizophrenia 1 Interactome: evidence for the close connectivity of risk genes and a potential synaptic basis for schizophrenia. Molecular psychiatry. 2007; 12:74–86. [PubMed: 17043677]

Carlisle HJ, Fink AE, Grant SG, O'Dell TJ. Opposing effects of PSD-93 and PSD-95 on long-term potentiation and spike timing-dependent plasticity. J Physiol. 2008; 586:5885–5900. [PubMed: 18936077]

Chae JH, Stein GH, Lee JE. NeuroD: the predicted and the surprising. Mol Cells. 2004; 18:271–288. [PubMed: 15650322]

Clelland CD, Choi M, Romberg C, Clemenson GD Jr, Fragniere A, Tyers P, Jessberger S, Saksida LM, Barker RA, Gage FH, Bussey TJ. A functional role for adult hippocampal neurogenesis in spatial pattern separation. Science. 2009; 325:210–213. [PubMed: 19590004]

Coba MP, Pocklington AJ, Collins MO, Kopanitsa MV, Uren RT, Swamy S, Croning MD, Choudhary JS, Grant SG. Neurotransmitters drive combinatorial multistate postsynaptic density networks. Science signaling. 2009; 2:ra19. [PubMed: 19401593]

Creer DJ, Romberg C, Saksida LM, van Praag H, Bussey TJ. Running enhances spatial pattern separation in mice. Proceedings of the National Academy of Sciences of the United States of America. 2010; 107:2367–2372. [PubMed: 20133882]

DeCarolis NA, Eisch AJ. Hippocampal neurogenesis as a target for the treatment of mental illness: a critical evaluation. Neuropharmacology. 2010; 58:884–893. [PubMed: 20060007]

Du P, Kibbe WA, Lin SM. lumi: a pipeline for processing Illumina microarray. Bioinformatics. 2008; 24:1547–1548. [PubMed: 18467348]

Edgar PF, Douglas JE, Cooper GJ, Dean B, Kydd R, Faull RL. Comparative proteome analysis of the hippocampus implicates chromosome 6q in schizophrenia. Molecular psychiatry. 2000; 5:85–90. [PubMed: 10673773]

Elia J, et al. Genome-wide copy number variation study associates metabotropic glutamate receptor gene networks with attention deficit hyperactivity disorder. Nature genetics. 2012; 44:78–84. [PubMed: 22138692]

Fernandez E, Collins MO, Uren RT, Kopanitsa MV, Komiyama NH, Croning MD, Zografos L, Armstrong JD, Choudhary JS, Grant SG. Targeted tandem affinity purification of PSD-95 recovers core postsynaptic complexes and schizophrenia susceptibility proteins. Mol Syst Biol. 2009; 5:269. [PubMed: 19455133]

Gao X, Arlotta P, Macklis JD, Chen J. Conditional knock-out of beta-catenin in postnatal-born dentate gyrus granule neurons results in dendritic malformation. J Neurosci. 2007; 27:14317–14325. [PubMed: 18160639]

Gao Z, Ure K, Ables JL, Lagace DC, Nave KA, Goebbels S, Eisch AJ, Hsieh J. Neurod1 is essential for the survival and maturation of adult-born neurons. Nature neuroscience. 2009; 12:1090–1092.

Gilbert PE, Kesner RP, Lee I. Dissociating hippocampal subregions: double dissociation between dentate gyrus and CA1. Hippocampus. 2001; 11:626–636. [PubMed: 11811656]

Grove EA, Tole S, Limon J, Yip L, Ragsdale CW. The hem of the embryonic cerebral cortex is defined by the expression of multiple Wnt genes and is compromised in Gli3-deficient mice. Development. 1998; 125:2315–2325. [PubMed: 9584130]

Guo W, Murthy AC, Zhang L, Johnson EB, Schaller EG, Allan AM, Zhao X. Inhibition of GSK3beta improves hippocampus-dependent learning and rescues neurogenesis in a mouse model of fragile X syndrome. Hum Mol Genet. 2011; 21:681–691. [PubMed: 22048960]

Hansen T, et al. At-Risk Variant in TCF7L2 for Type II Diabetes Increases Risk of Schizophrenia. Biological psychiatry. 2011

Huang da W, Sherman BT, Lempicki RA. Systematic and integrative analysis of large gene lists using DAVID bioinformatics resources. Nat Protoc. 2009; 4:44–57. [PubMed: 19131956]

Hunsaker MR, Kesner RP. Evaluating the differential roles of the dorsal dentate gyrus, dorsal CA3, and dorsal CA1 during a temporal ordering for spatial locations task. Hippocampus. 2008; 18:955–964. [PubMed: 18493930]

Hur EM, Zhou FQ. GSK3 signalling in neural development. Nature reviews Neuroscience. 2010; 11:539–551.

Husi H, Ward MA, Choudhary JS, Blackstock WP, Grant SG. Proteomic analysis of NMDA receptor-adhesion protein signaling complexes. Nature neuroscience. 2000; 3:661–669.

Hussain NK, Hsin H, Huganir RL, Sheng M. MINK and TNIK Differentially Act on Rap2-Mediated Signal Transduction to Regulate Neuronal Structure and AMPA Receptor Function. J Neurosci. 2010; 30:14786–14794. [PubMed: 21048137]

Ishizuka K, Kamiya A, Oh EC, Kanki H, Seshadri S, Robinson JF, Murdoch H, Dunlop AJ, Kubo KI, Furukori K, Huang B, Zeledon M, Hayashi-Takagi A, Okano H, Nakajima K, Houslay MD, Katsanis N, Sawa A. DISC1-dependent switch from progenitor proliferation to migration in the developing cortex. Nature. 2011

Jope RS, Roh MS. Glycogen synthase kinase-3 (GSK3) in psychiatric diseases and therapeutic interventions. Curr Drug Targets. 2006; 7:1421–1434. [PubMed: 17100582]

Kawabe H, Neeb A, Dimova K, Young SM Jr, Takeda M, Katsurabayashi S, Mitkovski M, Malakhova OA, Zhang DE, Umikawa M, Kariya K, Goebbels S, Nave KA, Rosenmund C, Jahn O, Rhee J, Brose N. Regulation of Rap2A by the ubiquitin ligase Nedd4-1 controls neurite development. Neuron. 2010; 65:358–372. [PubMed: 20159449]

Kee N, Sivalingam S, Boonstra R, Wojtowicz JM. The utility of Ki-67 and BrdU as proliferative markers of adult neurogenesis. J Neurosci Methods. 2002; 115:97–105. [PubMed: 11897369]

Kirov G, et al. De novo CNV analysis implicates specific abnormalities of postsynaptic signalling complexes in the pathogenesis of schizophrenia. Molecular psychiatry. 2011

Kopanitsa MV, Afinowi NO, Grant SG. Recording long-term potentiation of synaptic transmission by three-dimensional multi-electrode arrays. BMC Neurosci. 2006; 7:61. [PubMed: 16942609]

Kuwabara T, Hsieh J, Muotri A, Yeo G, Warashina M, Lie DC, Moore L, Nakashima K, Asashima M, Gage FH. Wnt-mediated activation of NeuroD1 and retro-elements during adult neurogenesis. Nat Neurosci. 2009; 12:1097–1105. [PubMed: 19701198]

Lee SM, Tole S, Grove E, McMahon AP. A local Wnt-3a signal is required for development of the mammalian hippocampus. Development. 2000; 127:457–467. [PubMed: 10631167]

Leutgeb JK, Leutgeb S, Moser MB, Moser EI. Pattern separation in the dentate gyrus and CA3 of the hippocampus. Science (New York, NY. 2007; 315:961–966.

Lin JW, Wyszynski M, Madhavan R, Sealock R, Kim JU, Sheng M. Yotiao, a novel protein of neuromuscular junction and brain that interacts with specific splice variants of NMDA receptor subunit NR1. The Journal of neuroscience: the official journal of the Society for Neuroscience. 1998; 18:2017–2027. [PubMed: 9482789]

Liu M, Pleasure SJ, Collins AE, Noebels JL, Naya FJ, Tsai MJ, Lowenstein DH. Loss of BETA2/NeuroD leads to malformation of the dentate gyrus and epilepsy. Proc Natl Acad Sci U S A. 2000; 97:865–870. [PubMed: 10639171]

Lu W, Shi Y, Jackson AC, Bjorgan K, During MJ, Sprengel R, Seeburg PH, Nicoll RA. Subunit composition of synaptic AMPA receptors revealed by a single-cell genetic approach. Neuron. 2009; 62:254–268. [PubMed: 19409270]

Luo Y, Shan G, Guo W, Smrt RD, Johnson EB, Li X, Pfeiffer RL, Szulwach KE, Duan R, Barkho BZ, Li W, Liu C, Jin P, Zhao X. Fragile x mental retardation protein regulates proliferation and differentiation of adult neural stem/progenitor cells. PLoS Genet. 2010; 6:e1000898. [PubMed: 20386739]

MacLaren EJ, Charlesworth P, Coba MP, Grant SG. Knockdown of mental disorder susceptibility genes disrupts neuronal network physiology in vitro. Mol Cell Neurosci. 2011; 47:93–99. [PubMed: 21440632]

Mahmoudi T, Li VS, Ng SS, Taouatas N, Vries RG, Mohammed S, Heck AJ, Clevers H. The kinase TNIK is an essential activator of Wnt target genes. Embo J. 2009; 28:3329–3340. [PubMed: 19816403]

Mao Y, Ge X, Frank CL, Madison JM, Koehler AN, Doud MK, Tassa C, Berry EM, Soda T, Singh KK, Biechele T, Petryshen TL, Moon RT, Haggarty SJ, Tsai LH. Disrupted in schizophrenia 1 regulates neuronal progenitor proliferation via modulation of GSK3beta/beta-catenin signaling. Cell. 2009; 136:1017–1031. [PubMed: 19303846]

McHugh TJ, Jones MW, Quinn JJ, Balthasar N, Coppari R, Elmquist JK, Lowell BB, Fanselow MS, Wilson MA, Tonegawa S. Dentate gyrus NMDA receptors mediate rapid pattern separation in the hippocampal network. Science (New York, NY. 2007; 317:94–99.

Min WW, Yuskaitis CJ, Yan Q, Sikorski C, Chen S, Jope RS, Bauchwitz RP. Elevated glycogen synthase kinase-3 activity in Fragile X mice: key metabolic regulator with evidence for treatment potential. Neuropharmacology. 2009; 56:463–472. [PubMed: 18952114]

Miyata T, Maeda T, Lee JE. NeuroD is required for differentiation of the granule cells in the cerebellum and hippocampus. Genes Dev. 1999; 13:1647–1652. [PubMed: 10398678]

Mohn AR, Gainetdinov RR, Caron MG, Koller BH. Mice with reduced NMDA receptor expression display behaviors related to schizophrenia. Cell. 1999; 98:427–436. [PubMed: 10481908]

Nakata K, Ujike H, Sakai A, Takaki M, Imamura T, Tanaka Y, Kuroda S. The human dihydropyrimidinase-related protein 2 gene on chromosome 8p21 is associated with paranoid-type schizophrenia. Biological psychiatry. 2003; 53:571–576. [PubMed: 12679234]

Pantelis C, Barber FZ, Barnes TR, Nelson HE, Owen AM, Robbins TW. Comparison of set-shifting ability in patients with chronic schizophrenia and frontal lobe damage. Schizophrenia research. 1999; 37:251–270. [PubMed: 10403197]

Potkin SG, Turner JA, Guffanti G, Lakatos A, Fallon JH, Nguyen DD, Mathalon D, Ford J, Lauriello J, Macciardi F. A genome-wide association study of schizophrenia using brain activation as a quantitative phenotype. Schizophr Bull. 2009; 35:96–108. [PubMed: 19023125]

Prickaerts J, Moechars D, Cryns K, Lenaerts I, van Craenendonck H, Goris I, Daneels G, Bouwknecht JA, Steckler T. Transgenic mice overexpressing glycogen synthase kinase 3beta: a putative model of hyperactivity and mania. The Journal of neuroscience: the official journal of the Society for Neuroscience. 2006; 26:9022–9029. [PubMed: 16943560]

Reif A, Schmitt A, Fritzen S, Lesch KP. Neurogenesis and schizophrenia: dividing neurons in a divided mind? Eur Arch Psychiatry Clin Neurosci. 2007; 257:290–299. [PubMed: 17468935]

Reif A, Fritzen S, Finger M, Strobel A, Lauer M, Schmitt A, Lesch KP. Neural stem cell proliferation is decreased in schizophrenia, but not in depression. Molecular psychiatry. 2006; 11:514–522. [PubMed: 16415915]

Sahay A, Scobie KN, Hill AS, O'Carroll CM, Kheirbek MA, Burghardt NS, Fenton AA, Dranovsky A, Hen R. Increasing adult hippocampal neurogenesis is sufficient to improve pattern separation. Nature. 2011

Scott JD, Pawson T. Cell signaling in space and time: where proteins come together and when they're apart. Science. 2009; 326:1220–1224. [PubMed: 19965465]

Shen S, Lang B, Nakamoto C, Zhang F, Pu J, Kuan SL, Chatzi C, He S, Mackie I, Brandon NJ, Marquis KL, Day M, Hurko O, McCaig CD, Riedel G, St Clair D. Schizophrenia-related neural and behavioral phenotypes in transgenic mice expressing truncated Disc1. The Journal of neuroscience: the official journal of the Society for Neuroscience. 2008; 28:10893–10904. [PubMed: 18945897]

Shi J, et al. Common variants on chromosome 6p22.1 are associated with schizophrenia. Nature. 2009; 460:753–757. [PubMed: 19571809]

Shitashige M, Satow R, Jigami T, Aoki K, Honda K, Shibata T, Ono M, Hirohashi S, Yamada T. Traf2- and Nck-interacting kinase is essential for Wnt signaling and colorectal cancer growth. Cancer Res. 2010; 70:5024–5033. [PubMed: 20530691]

Sirerol-Piquer M, Gomez-Ramos P, Hernandez F, Perez M, Moran MA, Fuster-Matanzo A, Lucas JJ, Avila J, Garcia-Verdugo JM. GSK3beta overexpression induces neuronal death and a depletion of the neurogenic niches in the dentate gyrus. Hippocampus. 2010

Smyth, G.; Ritchie, M.; Thorne, N.; Wettenhall, J.; Shi, W. limma: Linear Models for Microarray Data. 2005.

Talpos JC, Winters BD, Dias R, Saksida LM, Bussey TJ. A novel touchscreen-automated paired-associate learning (PAL) task sensitive to pharmacological manipulation of the hippocampus: a translational rodent model of cognitive impairments in neurodegenerative disease. Psychopharmacology (Berl). 2009; 205:157–168. [PubMed: 19357840]

Tamminga CA, Stan AD, Wagner AD. The hippocampal formation in schizophrenia. The American journal of psychiatry. 2010; 167:1178–1193. [PubMed: 20810471]

Toro CT, Deakin JF. Adult neurogenesis and schizophrenia: a window on abnormal early brain development? Schizophrenia research. 2007; 90:1–14. [PubMed: 17123784]

von Bohlen Und Halbach O. Immunohistological markers for staging neurogenesis in adult hippocampus. Cell Tissue Res. 2007; 329:409–420. [PubMed: 17541643]

Wang Q, et al. The psychiatric disease risk factors DISC1 and TNIK interact to regulate synapse composition and function. Molecular psychiatry. 2010:1–18. [PubMed: 20029403]

Wexler EM, Geschwind DH, Palmer TD. Lithium regulates adult hippocampal progenitor development through canonical Wnt pathway activation. Molecular psychiatry. 2008; 13:285–292. [PubMed: 17968353]

Zamanillo D, Sprengel R, Hvalby O, Jensen V, Burnashev N, Rozov A, Kaiser KM, Koster HJ, Borchardt T, Worley P, Lubke J, Frotscher M, Kelly PH, Sommer B, Andersen P, Seeburg PH, Sakmann B. Importance of AMPA receptors for hippocampal synaptic plasticity but not for spatial learning. Science. 1999; 284:1805–1811. [PubMed: 10364547]

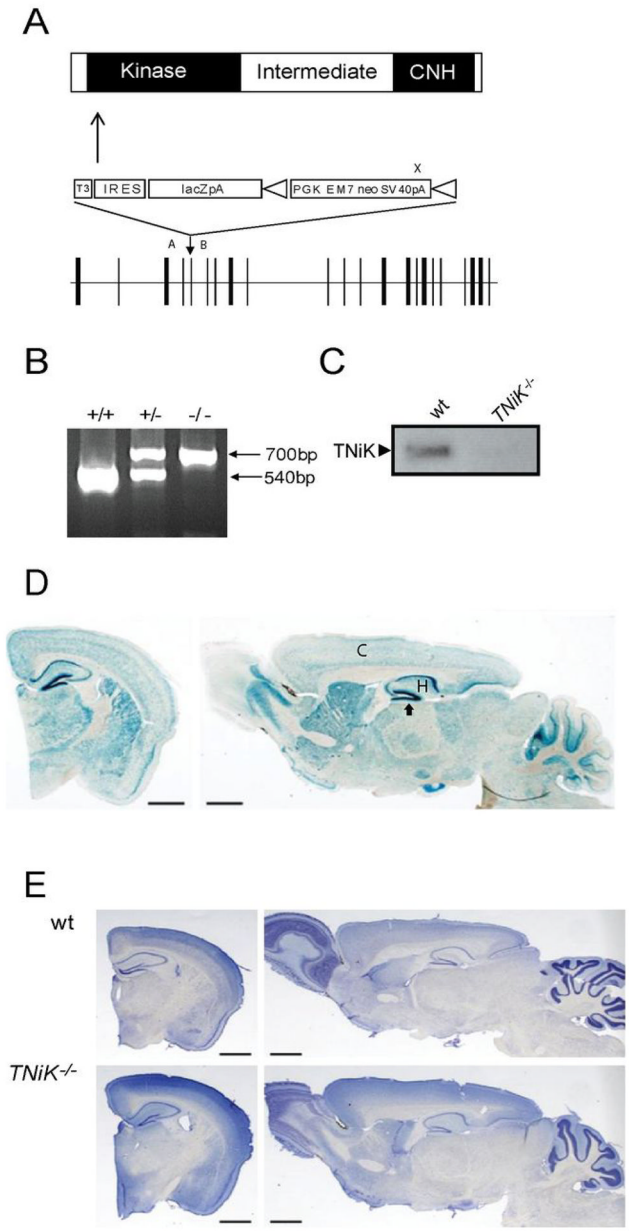

Figure 1. TNiK knockout mice

1A. Targeting vector for the generation of TNiK knockout mice. Linear structure of TNiK protein showing kinase, intermediate and citron homology (CNH) domain. Arrow indicates N-terminal point of targeted deletion and middle panel shows gene targeting vector containing the IRES-lacZ-neo reporter cassette and lower panel the genomic locus (exons; vertical bars). Vector sequences include: T3, triple termination sequence; IRES, internal ribosome entry sequence; LacZpA, β-galactosidase reporter with polyA sequence; triangles flanking PGKEM7neoSV40pA (selection cassette) are loxP recombination sites. PCR genotyping primer sites, A,B,X.

1B. Genotyping heterozygous and homozygous mice. A 540bp product was amplified from the wild-type (wt) allele using primers A and B and a 700bp product amplified from the targeted allele using primers B and X.

1C. Immunoblot with TNiK antibodies of total hippocampal lysates shows absence of TNiK protein in *TNiK*$^{-/-}$ mice.
1D. Brain expression of TNiK. Coronal and sagittal brain section stained with X-gal in *TNiK*$^{-/-}$ mice. C, cortex; H, hippocampus; arrow to dentate gyrus.
Scale bar: 1.4mm
1E. Coronal and sagittal brain sections stained with Nissl from adult wt and *TNiK*$^{-/-}$ mice.
Scale bar: 1.4mm

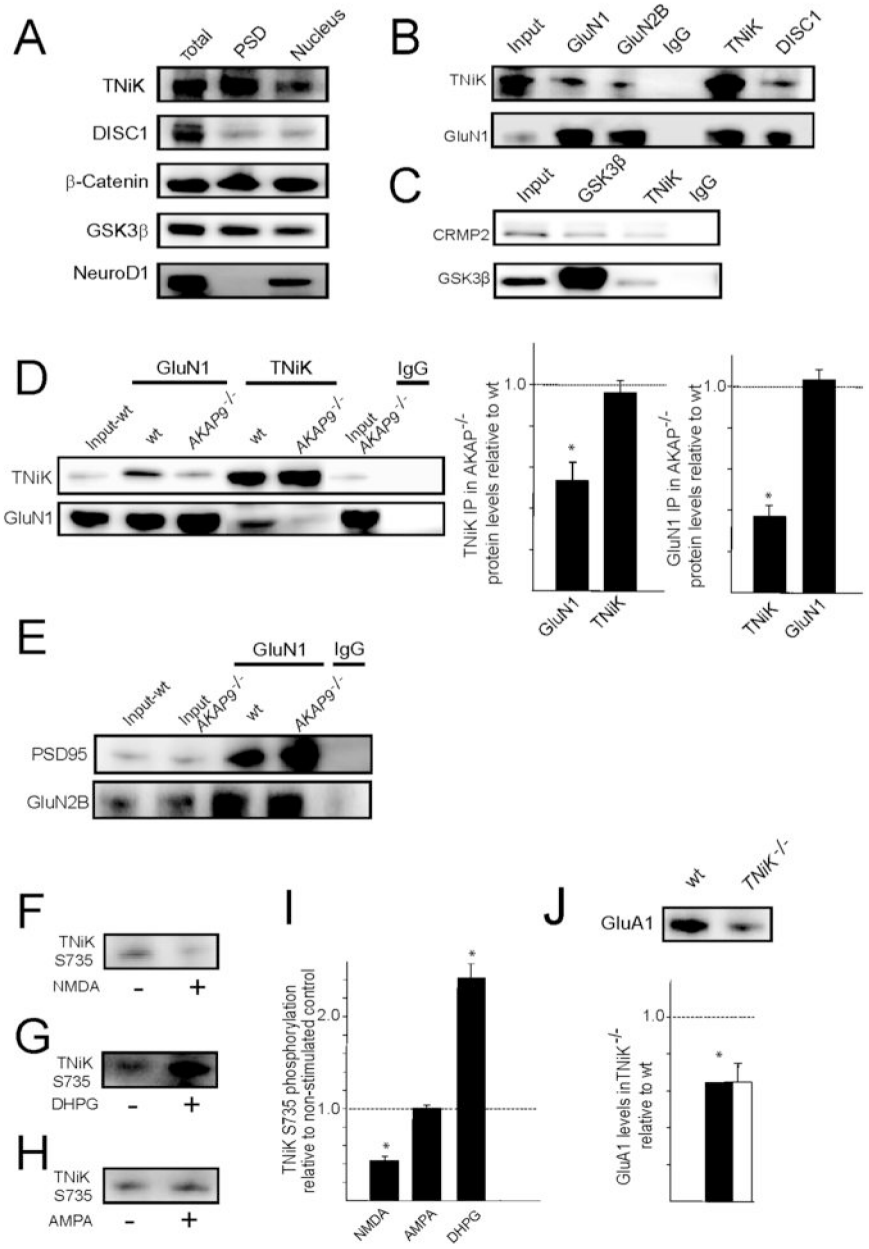

Figure 2. Postsynaptic TNiK complexes and increased GSK3β signalling in *TNiK*$^{-/-}$ mice

2A. Immunoblot showing TNiK, DISC1, β-catenin, and GSK3β in total hippocampal lysates, PSD and nucleus fraction. The transcription factor NeuroD1 was found only in the nuclear fraction and absent from the PSD.

2B. TNiK, NMDAR and DISC1 complexes. PSD lysates (input) were immunoprecipitated with antibodies to GluN1, GLuN2B, TNiK, DISC1 and control IgG (labels above the blots) and immunoblotted with antibodies to TNiK and GluN1 (labels to left of blots).

2C. TNiK, CRMP2 and GSK3β complexes. PSD lysates were immunoprecipitated with antibodies to TNiK, GSK3β and control IgG and immunoblotted with antibodies to CRMP2 and GSK3β. Labelled as in 2B.

2D. Immunoprecipitation with GluN1 antibodies and control IgG, and western blot against TNiK in wt and *AKAP9*$^{-/-}$ mice (left panel) showed a 52% reduction ($p<0.05$) (right panel).

Reciprocal immunoprecipitation with TNiK and GluN1 antibodies and western blot against GluN1 in wt and AKAP9 mutant mice (left panel) observed a 63% reduction ($p<0.05$)(right panel). The total levels of TNiK and GluN1 were not altered in *AKAP9*$^{-/-}$ mice (lane 1 and 6).

2E. Unaltered GluN1, GluN2B, PSD95 complexes in *AKAP9*$^{-/-}$ mice. Wt and AKAP9 mutant input extracts are indicated and immunoprecipitating antibody is shown above the blot.

2F–I. Glutamate receptors modulate bidirectional phosphorylation of TNiK.

2F. TNiK S735 phosphorylation measured by immunoblot of PSD lysates from hippocampus slices stimulated with NMDA.

2G. TNiK S735 phosphorylation measured by immunoblot of PSD lysates from hippocampus slices stimulated with the metabotropic agonist DHPG.

2H. TNiK S735 phosphorylation measured by immunoblot of PSD lysates from hippocampus slices stimulated with AMPA.

2I. NMDAR activation in hippocampal slices decreases TNiK S735 phosphorylation, activation of metabotropic glutamate receptors type I (mGluRI) with DHPG produced an increase in S735 phosphorylation, while AMPA activation had no effect.

2J. PSD lysates were immunoblotted with antibody to GluA1. Histogram shows 35% decrease ($p<0.05$).

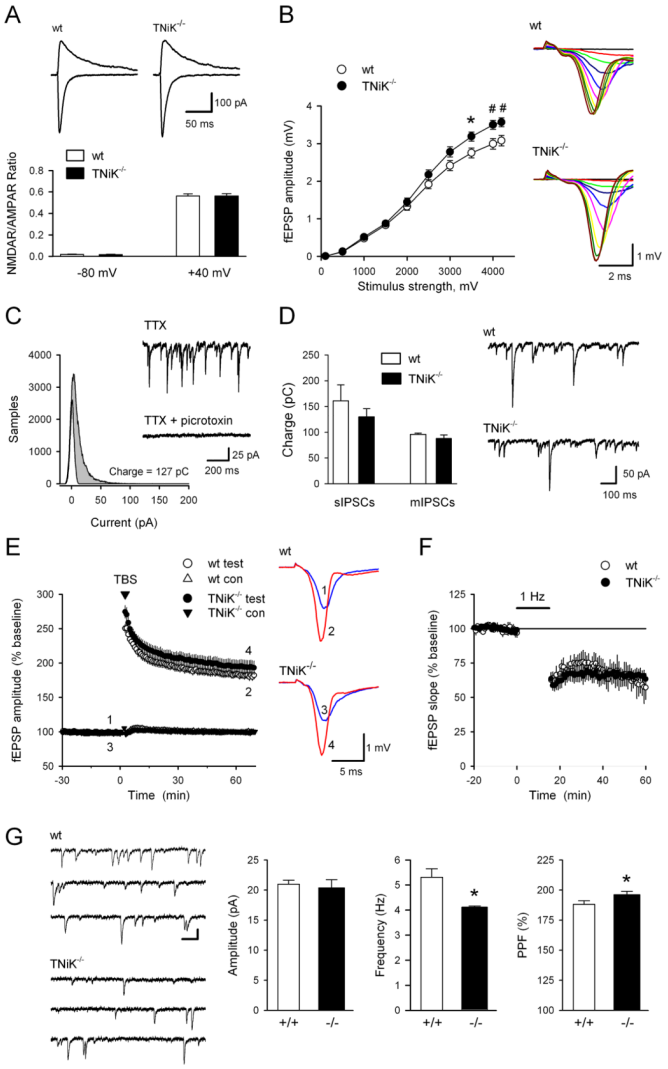

Figure 3. Synaptic physiology in *TNiK*$^{-/-}$ mice

3A. NMDA receptor-mediated EPSCs are normal in *TNiK*$^{-/-}$ mice. Traces (top) show EPSCs recorded at −80 and +40 mV in pyramidal cells from a wt (left) and *TNiK*$^{-/-}$ mouse (right). Calibration bars are 100 pA and 25 msec. The ratios of NMDA receptor-mediated EPSCs to AMPA receptor-mediated EPSCs measured at −80 and +40 mV (bottom) are not significant different in *TNiK*$^{-/-}$ mice (n = 17; N = 3) compared to wt littermates (n = 17; N = 3).

3B. Baseline synaptic transmission was slightly but significantly enhanced in *TNiK*$^{-/-}$ mice. Input-output relationships illustrate averaged fEPSP amplitudes in slices from *TNiK*$^{-/-}$ (n = 28; N = 10) and wt mice (n = 32; N = 10) in response to stimulation of Schäffer collaterals by biphasic voltage pulses of 0.1 – 4.2 V (*p < 0.05, #p < 0.01). Amplitudes of fEPSPs evoked by maximum 4.2V stimulation were significantly increased in TNiK mice ($F_{(1,40)}$=9.18; P = 0.004, two-way nested ANOVA, main genotype effect). Representative families of fEPSP traces are shown at right. Calibration bars are 1 mV and 2 msec.

3C. Spontaneously occurring IPSCs were recorded in cells voltage-clamped at −70 and all-points histograms were generated from 10 sec long segments of data. Points corresponding to baseline noise were estimated from the Gaussian curve centered on 0 pA. The difference between this area and the remaining area under the histogram corresponds to the currents

generated by the IPSCs (shaded area) and was used to calculate total charge transfer. Traces show mIPSCs recorded before and after bath application of picrotoxin (100 μM).

3D. Comparison of spontaneous and miniature IPSC charge transfer in wt (open bars) and *TNiK*$^{-/-}$ cells (filled bars). Spontaneous IPSCs (recorded in the absence of TTX) in cells from TNiK−/− mice (n = 10 cells from 4 mice) are not significantly different from that seen in wt cells (n = 10 cells from 4 mice, p = 0.41). Total charge transfer due to mIPSCs is also similar in *TNiK*$^{-/-}$ (n = 13 cells from 4 mice) and wt mice (n = 15 cells from 3 mice, p = 0.39). Traces show sIPSCs recorded from CA1 pyramidal cells in slices from wt and *TNiK*$^{-/-}$ mice.

3E. Theta-burst stimulation elicited pathway-specific long-term potentiation of synaptic transmission in hippocampus CA1 area. Normalised magnitude of this potentiation 60–65 min after LTP induction was identical in mutant mice (189 ± 5%; n = 28; N = 10; P = 0.94) and their wt littermates (189 ± 4%; n = 32; N = 10). Traces show examples of test pathway fEPSPs evoked immediately before and 1 h after theta-burst stimulation.

3F. Hippocampal long-term depression induced by 1 Hz stimulation (900 pulses) is normal in *TNiK*$^{-/-}$ mice. 45 minutes post-1 Hz stimulation fEPSPs were reduced to 65 ± 4% of baseline in slices from *TNiK*$^{-/-}$ mice (n = 11; N = 5) compared to 60 ± 9% of baseline in slices from wt mice (n = 5; N = 3).

3G. Frequency of spontaneous mEPSCs is significantly reduced in *TNiK*$^{-/-}$ mice. Traces (left) show consecutive sweeps of mEPSCs recorded in a wt cell (top, n = 14; N = 3) and a *TNiK*$^{-/-}$ cell (bottom, n = 14; N = 3). Calibration bars are 100 ms and 15 pA. Histograms (right) show the amplitude, and frequency of mEPSPs as well as paired-pulse facilitation (PPF) of fEPSPs (50 msec inter-pulse interval) in *TNiK*$^{-/-}$ mice compared to wt mice (*p < 0.05).

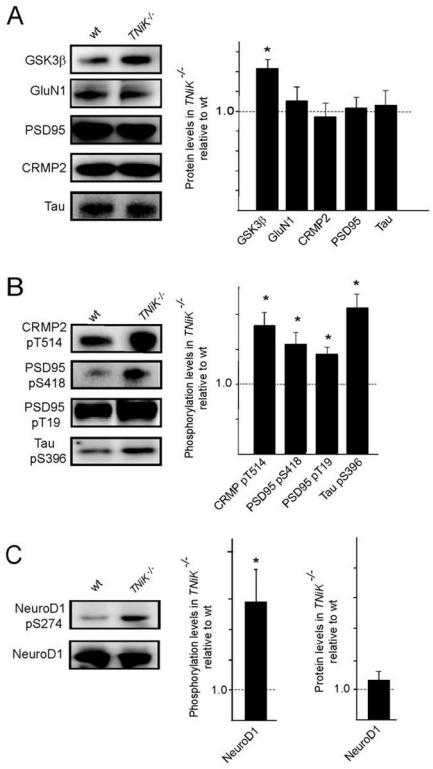

Figure 4. Elevated GSK3β levels in *TNiK*$^{-/-}$ mice

4A. Immunoblots of GSK3β, GluN1, PSD-95, CRMP2, and Tau in PSD lysates from wt and *TNiK*$^{-/-}$ mice. Histograms shows proteins level in *TNiK*$^{-/-}$ mice PSD normalised to wt levels.

4B. PSD lysates were immunoblotted with phosphospecific antibodies showing increased phosphorylation of CRMP2 threonine 514, PSD-95 serine 418 and threonine 19, and tau serine 396 in *TNiK*$^{-/-}$ mice.

4C. Hippocampal lysates were immunoblotted with phosphospecific antibodies to serine 294 on NeuroD1 (upper panel) and total NeuroD1 (lower panel) and levels in *TNiK*$^{-/-}$ mice quantified relative to wt in histograms.

Images shows representative western blot assays from at least triplicate experiments. Asterisk indicates significant difference to wt ($p<0.05$).

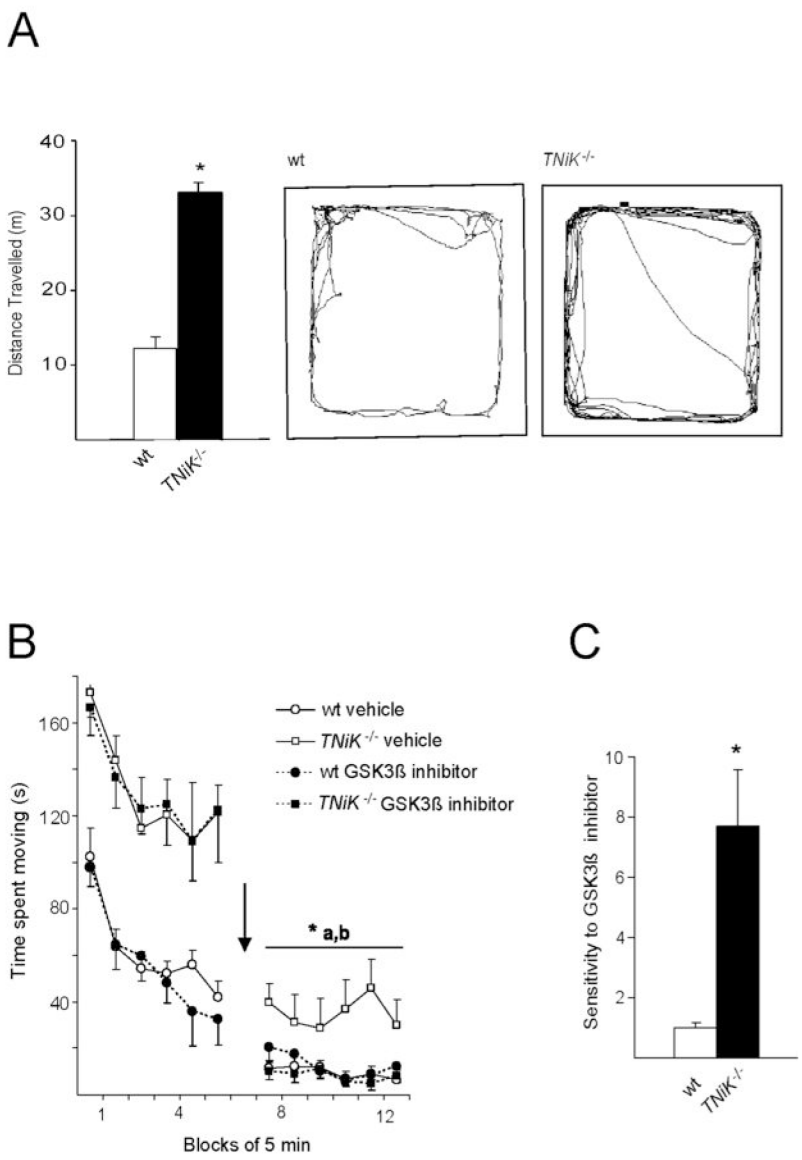

Figure 5. Inhibition of GSK3β reverses hyperactivity in *TNiK*$^{-/-}$ mice

5A–C. Locomotor activity was assessed in an open field chamber and total distance moved measured (5A). Representative tracks of wt (5A-left) and *TNiK*$^{-/-}$ (5A-right) mice in the open field. GSK3β inhibition on locomotor activity (5B) was assessed by placing *TNiK*$^{-/-}$ and wt mice in an activity chamber for an initial period of 30 min, then mice were injected (indicated by arrow) with either vehicle or a GSK3β inhibitor (SB 216763, 10 mg/kg of body weight i.p.) and monitored for a further period of 30 min starting 10 min after injection. Sensitivity to GSK3β (5C) was calculated as a ratio of change in locomotor activity between administration of vehicle and GSK3β inhibitor. *p<0.05; **p<0.01; ***p<0.005; a = *TNiK*$^{-/-}$ vehicle vs. wt vehicle, b = *TNiK*$^{-/-}$ vehicle vs. *TNiK*$^{-/-}$ GSK3β inhibitor.

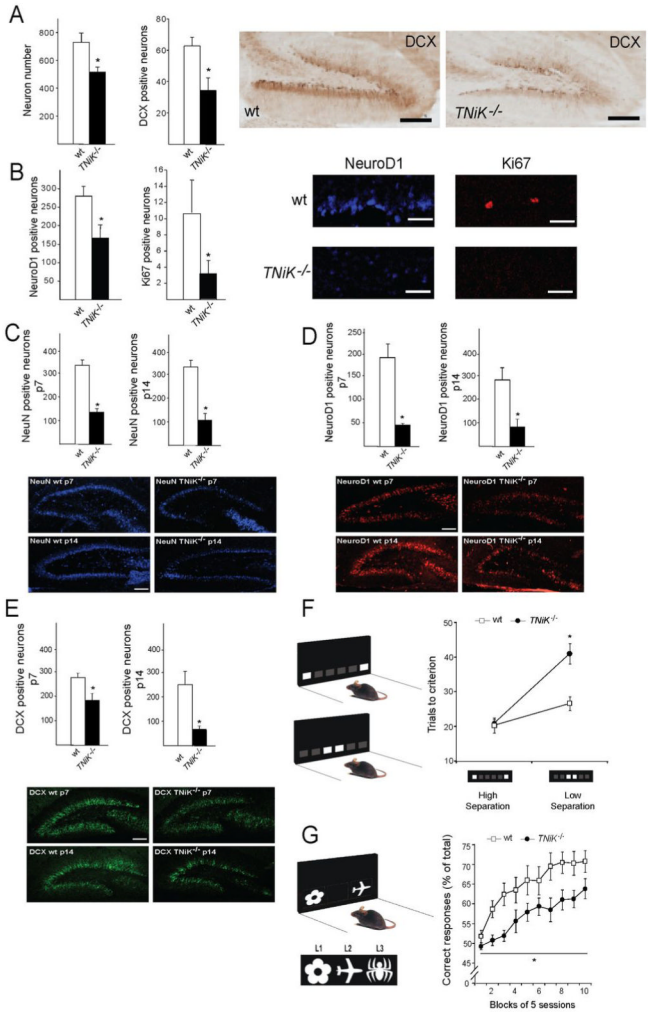

Figure 6. Impaired dentate gyrus neurogenesis and cognition in *TNiK*$^{-/-}$ mice

6A,B. Histograms comparing dentate gyrus granule cell number and cells stained with markers relevant to neurogenesis (see text) in wt and *TNiK*$^{-/-}$ mice brain sections. Representative images of dentate gyrus cells in wt and *TNiK*$^{-/-}$ brain sections stained with markers for DCX (6A), NeuroD1 and Ki67 (6B). Scale bars:200μm; 60μm.

6C–E. Hippocampus development in *TNiK*$^{-/-}$mice. Number of NeuN positive neurons at P7 (left histogram, upper two panels of immunohistochemistry) and P14 (right histogram, lower two panels of immunohistochemistry) in wt and *TNiK*$^{-/-}$ mice (6C). Number of NeuroD1 positive neurons at P7 (left histogram, upper two panels of immunohistochemistry) and P14 (right histogram, lower two panels of immunohistochemistry) in wt and *TNiK*$^{-/-}$ mice (6D). Number of DCX positive neurons at P7 (left histogram, upper two panels of immunohistochemistry) and P14 (right histogram, lower two panels of immunohistochemistry) in wt and *TNiK*$^{-/-}$ mice (6E). Scale bars: 100μm.

6F. Pattern separation was assessed using a two-choice spatial discrimination task in the touchscreen-based operant system. Mice were trained to discriminate the correct spatial location between two illuminated squares, located in two out of six possible locations. Pattern separation was tested by varying the distance between the choice locations, either situated far apart (high degree of separation)(upper panel) or close together (low degree of separation) (lower panel). *TNiK*$^{-/-}$mice performed as well as wt mice when stimuli were separated by a high degree of separation, however, showed a significant impairment

($p<0.05$) in discrimination when the locations were in close proximity. As a control measure, analysis of response reaction times showed no significant differences between groups at either separation (High separation, wt = 5.0 ± 1.1 s, *TNiK*$^{-/-}$ = 5.2 ± 0.8s; Low separation, wt = 4.9 ± 0.7s, *TNiK*$^{-/-}$ =5.0 ± 0.9s).

6G. *TNiK*$^{-/-}$ mice show a deficit in object-location associative learning (significant effect of genotype, $p<0.05$) where mice were tested for the ability to associate between three objects (flower, plane, and spider) with their correct spatial locations on the screen (left (L1), middle (L2), and right (L3), respectively).

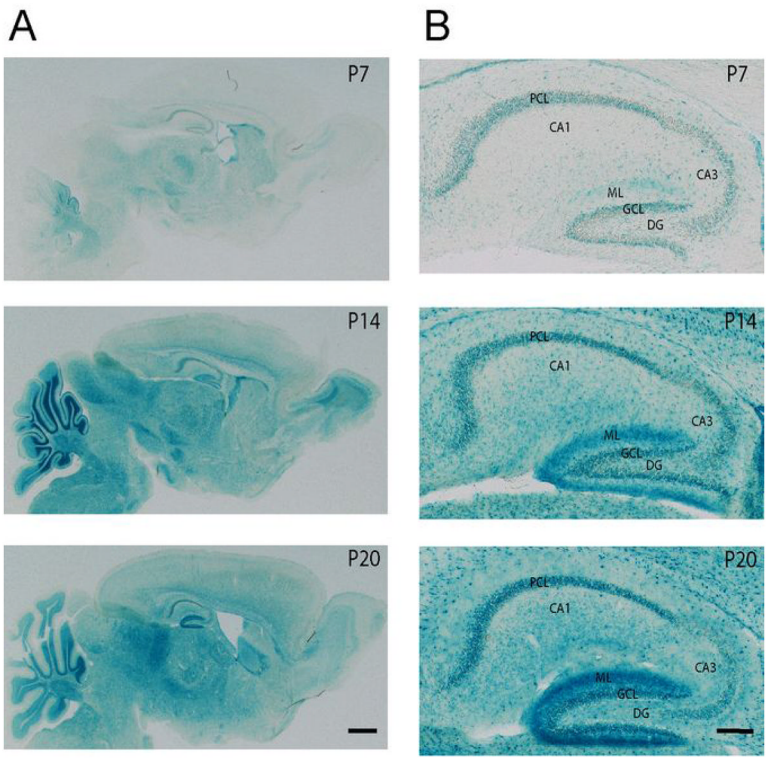

Figure 7. Postnatal expression profile of TNiK

7A. Saggital sections showing expression pattern of TNiK using X-Gal staining in *TNiK*$^{-/-}$ mice at postnatal day 7, 14 and 20. Scale bar: 100μm

7B. Detailed expression pattern of TNiK using X-Gal staining of hippocampal area. Scale bar: 200μm. Dentate gyrus (DG), granule cell layer (GCL), molecular layer (ML), pyramidal cell layer (PCL).

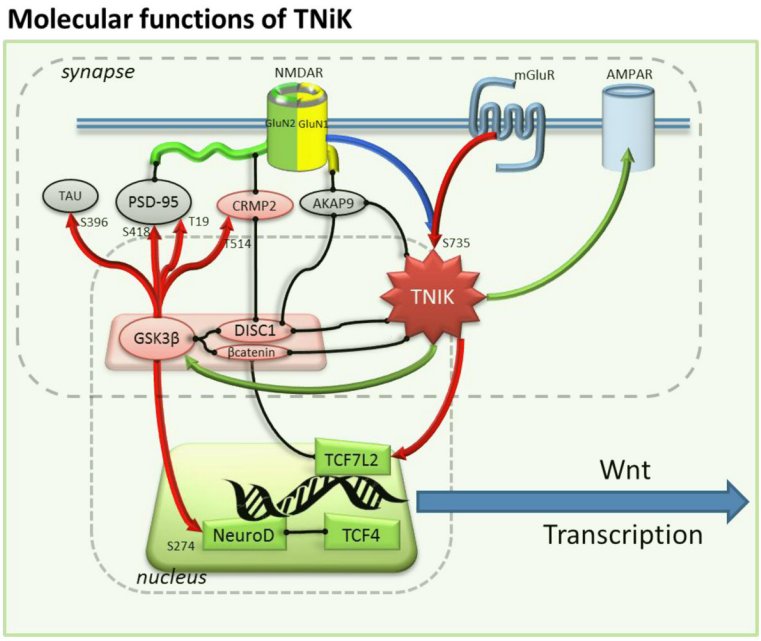

Figure 8. Molecular functions of TNiK

The molecular functions of TNiK in the postsynaptic density and nucleus are shown. Proteins are shown as colored shapes and grouped into their synaptic and nuclear locations. Black lines connecting proteins show known protein-protein interactions; arrows show regulatory interactions: red, phosphorylation (phosphorylated amino acid residue indicated with number and letter); blue, dephosphorylation; green, regulates protein level.